

INVASION OF LESION TERRITORY BY REGENERATING FIBERS AFTER SPINAL CORD INJURY IN ADULT MACAQUE MONKEYS

M.-L. BEAUD,^a E. M. ROUILLER,^a J. BLOCH,^c A. MIR,^d
M. E. SCHWAB,^b T. WANNIER^{a,b} AND E. SCHMIDLIN^{a,*}

^a Department of Medicine and Program in Neurosciences,
Faculty of Sciences and Fribourg Center for Cognition,
University of Fribourg, Chemin du Musée 5, CH-1700
Fribourg, Switzerland

^b Brain Research Institute, Department of Neuromorphology,
University and ETH Zurich, Winterthurerstrasse 190, CH-8057 Zürich,
Switzerland

^c Department of Neurosurgery, Neurosurgery Clinic, University
Hospital of Lausanne, Rue du Bugnon, CH-1011 Lausanne,
Switzerland

^d Neuroscience Research, Novartis Institute for BioMedical Research,
CH-4002 Basel, Switzerland

Abstract—In adult macaque monkeys subjected to an incomplete spinal cord injury (SCI), corticospinal (CS) fibers are rarely observed to grow in the lesion territory. This situation is little affected by the application of an anti-Nogo-A antibody which otherwise fosters the growth of CS fibers rostrally and caudally to the lesion. However, when using the Sternberger monoclonal-incorporated antibody 32 (SMI-32), a marker detecting a non-phosphorylated neurofilament epitope, numerous SMI-32-positive (+) fibers were observed in the spinal lesion territory of 18 adult macaque monkeys; eight of these animals had received a control antibody infusion intrathecally for 1 month after the injury, five animals an anti-Nogo-A antibody, and five animals received an anti-Nogo-A antibody together with brain-derived neurotrophic factor (BDNF). These fibers occupied the whole dorso-ventral axis of the lesion site with a tendency to accumulate on the ventral side, and their trajectories were erratic. Most of these fibers (about 87%) were larger than 1.3 μm and densely SMI-32 (+) stained. In the undamaged spinal tissue, motoneurons form the only large population of SMI-32 (+) neurons which are densely stained and have large diameter axons. These data therefore suggest that a sizeable proportion of the fibers seen in the lesion territory originate from motoneurons, although fibers of other origins could also contribute. Neither the presence of the antibody neutralizing Nogo-A alone, nor the presence of the antibody neutralizing Nogo-A combined with BDNF influenced the number or the length of the SMI-32 (+) fibers in the spinal lesion area. In summary, our data show that after a spinal cord lesion in adult monkeys,

the lesion site is colonized by fibers, a large portion of which presumably originate from motoneurons.
© 2012 IBRO. Published by Elsevier Ltd. All rights reserved.

Key words: spinal cord lesion, scar tissue, primate, regeneration, BDNF, Nogo-A.

INTRODUCTION

In the adult central nervous system (CNS) of mammals, axotomized nerve fibers fail to regenerate over long distances. Among the factors contributing to this failure, the development of a scar tissue at the lesion site leads to the formation of an environment hostile to nerve fibers' regrowth and acting as a barrier against axonal regeneration into and across the lesion territory. Indeed, the scar tissue contains various neurite growth-inhibiting factors produced by cells such as microglial cells, meningeal cells, astrocytes or oligodendrocytes (Reier et al., 1983; Schwab and Bartholdi, 1996; Schwab, 2002; David and Lacroix, 2003). These last years, several growth-inhibiting molecules expressed in the scar tissue were identified such as the chondroitin sulfate proteoglycans (CSPGs), tenascin-c or semaphorins (Rudge and Silver, 1990; McKeon et al., 1991; Davies et al., 1997, 1999; Fawcett and Asher, 1999; Pasterkamp and Verhaagen, 2001). Nogo-A present in CNS myelin and oligodendrocytes inhibits the regeneration of spinal-lesioned axons (Schwab, 2004, 2010). In rodents, the application at the level of the spinal cord of an antibody neutralizing Nogo-A promotes both corticospinal (CS) fibers regeneration and functional recovery (Schnell and Schwab, 1990; Thallmair et al., 1998; Schwab, 2004; Liebscher et al., 2005; Maier et al., 2009). Experiments conducted on primates lead to similar results (Freund et al., 2006, 2007, 2009). In particular, these experiments have shown that in anti-Nogo-A antibody-treated monkeys, CS fibers sprout and regenerate rostrally, around and caudally to the spinal lesion (Fouad et al., 2004; Freund et al., 2006, 2007). However, in these animals, CS fibers were only exceptionally observed inside the lesion territory. Nevertheless, it remains possible that following spinal cord injury (SCI), neurons distinct from CS neurons show an ability to regenerate and to grow in or even through the scar tissue.

Neurofilaments constitute the main structural element of the neuronal cytoskeleton and the presence in neurons of non-phosphorylated forms of neurofilaments can be shown using the Sternberger monoclonal-incorporated

*Corresponding author. Address: Unit of Physiology, Department of Medicine, University of Fribourg, Chemin du Musée 5, CH-1700 Fribourg, Switzerland. Tel: +41-26-300-86-09; fax: +41-26-300-96-75.

E-mail address: eric.schmidlin@unifr.ch (E. Schmidlin).

Abbreviations: BDNF, brain-derived neurotrophic factor; CS, corticospinal; CSPGs, chondroitin sulfate proteoglycans; PBS, phosphate-buffered saline; SMI-32, Sternberger monoclonal-incorporated antibody 32.

Table 1. Individual characteristics and summary data for all animals included in the study

Name	Mk-CB	Mk-CBo	Mk-CC	Mk-CGa	Mk-CG	Mk-CH	Mk-CP	MK-CS		
	1,2,3,4	–	1,3	–	1,2,3,4	1,2,3,4	1,2,3	1,3,4		
Species	Fasc.	Fasc.	Mul.	Fasc.	Fasc.	Fasc.	Fasc.	Mul.		
Sex	♀	♂	♂	♂	♂	♂	♀	♂		
mAB received	Control									
Amount mAB (mg)	80	14	14.8	14	36	36	14.8	14.8		
BDNF treatment	No									
Amount BDNF (mg)	–	–	–	–	–	–	–	–		
BDA transport time (days)	78	99	21	87	70	62	78	35		
Lesion to BDA injection delay (days)	147	93	86	69	70	76	81	167		
Hemisection extent (%)	75	93	38	73	51	90	45	63		
Functional recovery (%)	78	99	83	100	90	53	83	22		
Age of the animal at the sacrifice (years)	5	~4	~4	~4	~4	~4	6.9	4.5		
Nb. fibers with $\varnothing < 1.3 \mu\text{m}$	266	190	64	83	34	232	143	24		
Nb. fibers with $\varnothing > 1.3 \mu\text{m}$	780	884	305	989	404	2307	657	158		
Nb. fibers in the lesion territory	1046	1074	369	1072	438	2539	800	182		
Cumulative length for fibers with $\varnothing < 1.3 \mu\text{m}$	13.6	21.6	4.5	6.0	3.1	21.9	20.5	2.7		
Cumulative length for fibers with $\varnothing > 1.3 \mu\text{m}$	63.0	94.0	27.6	72.6	31.2	178.9	86.5	18.9		
Cumulative length for all fibers in the lesion	76.5	115.6	32.0	78.6	34.3	200.8	107.0	21.6		
Volume of BDA injection (in μl)	20			34.5	24	20	24			
Nb. of BDA injection sites	10			21	12	10	12			
Name	Mk-AC	Mk-AF	Mk-AG	Mk-AK	Mk-AM	Mk-ABB	Mk-ABMa	Mk-ABMx	Mk-ABP	Mk-ABS
	1,2,3,4	1,3,4	2,4	3	1,2,3,4	–	–	–	–	–
Species	Fasc.	Mul.	Fasc.	Fasc.	Fasc.	Fasc.	Fasc.	Fasc.	Fasc.	Fasc.
Sex	♂	♂	♂	♂	♂	♂	♂	♂	♂	♂
mAB received	hNogoA	11C7	hNogoA	hNogoA	hNogoA	hNogoA	hNogoA	hNogoA	hNogoA	hNogoA
Amount mAB (mg)	36	14.8	14.6	36	36	36	36	36	36	36
BDNF treatment	No	No	No	No	No	Yes	Yes	Yes	Yes	Yes
Amount BDNF (mg)	–	–	–	–	–	1.4	1.4	1.4	1.4	1.4
BDA transport time (days)	64	71	70	62	69	76	65	79	69	62
Lesion to BDA injection delay (days)	71	187	42	90	69	91	84	179	111	111
Hemisection extent (%)	85	56	78	86	80	83	94	95	77	93
Functional recovery (%)	100	57	100	100	96	93	68	78	70	66
Age of the animal at the sacrifice (years)	~4	6.25	3.5	3.5	~4	5	~4	5	4.5	4.5
Nb. fibers with $\varnothing < 1.3 \mu\text{m}$	73	47	46	301	145	32	49	124	705	328
Nb. fibers with $\varnothing > 1.3 \mu\text{m}$	821	82	94	505	1607	526	918	1017	1199	953
Nb. fibers in the lesion territory	894	129	140	806	1752	558	967	1141	1904	1281
Cumulative length for fibers with $\varnothing < 1.3 \mu\text{m}$	6.6	4.7	3.2	26.2	17.5	4.6	3.1	12.3	41.2	23.6
Cumulative length for fibers with $\varnothing > 1.3 \mu\text{m}$	59.9	4.3	8.3	75.9	131.3	56.3	77.2	93.4	88.0	67.9
Cumulative length for all fibers in the lesion	66.5	9.0	11.5	102.1	148.8	60.9	80.4	105.7	129.2	91.5
Volume of BDA injection (in μl)	20		28		19	26	28.5	34.5		
Nb. of injection sites	10		15		10	12	19	27		

- 1 Nat Med 12 (2006) 790–792
- 2 JCN 502 (2007) 644–659
- 3 EJN 29 (2009) 983–996
- 4 Brain Res 1217 (2008) 96–109

At the time of the experiment, each monkey was assigned an identification code that did not allow experimenters to determine whether the animal was infused with the control antibody, with the anti-Nogo-A antibody or with the combination of the BDNF with the anti-Nogo-A antibody. New identification codes were assigned to the monkeys during the writing of the manuscript to improve its readability. The entry "reference" indicates whether some data have appeared in previous reports of our group: 1: Freund et al. (2006); 2: Freund et al. (2007); 3: Freund et al. (2009); 4: Wannier-Morino et al. (2008). Under species, "fasc." is for *Macaca fascicularis* and "mul." is for *Macaca mulatta*. Functional recovery (expressed in % for the behavioral parameter "score") was assessed here based on the modified Brinkman board task, by comparing the performance pre- and post-lesions (see e.g. Freund et al., 2009).

antibody 32 (SMI-32) (Sternberger and Sternberger, 1983; Lee et al., 1988). Inside the spinal cord, motoneurons present a strong SMI-32 immunoreactivity (Tsang et al., 2000). The goal of the present study was to investigate, using the SMI-32 antibody whether neurites can cross the scar tissue and colonize the lesion site and whether the anti-Nogo-A antibody treatment alone or combined with brain-derived neurotrophic factor (BDNF) can influence such regenerating nerve fibers.

EXPERIMENTAL PROCEDURES

Animals

Tissue material derived from 18 young adult macaques (3.5–6.9 years old; weight ranging from 3.0 to 5.0 kg), subjected to an incomplete spinal cord hemisection performed at cervical level C7/C8, was analyzed histologically. These animals were part of several studies on the consequences of anti-Nogo-A antibody treatment on the regeneration of CS axons as well as on behavioral recovery after cervical cord injury. Separate data from 10 of these animals have appeared in previous reports (Freund et al., 2006, 2007, 2009; Beaud et al., 2008; Wannier-Morino et al., 2008). Surgery and care of the animals were in conformity to the Guide for the Care and Use of Laboratory Animals (ISBN 0-309-05377-3; 1996) and authorized by local Swiss veterinary authorities. The housing conditions as well as the surgical procedures were reported in detail in earlier reports (Schmidlin et al., 2004, 2005; Freund et al., 2006, 2007, 2009). The experimental protocol can be summarized as follows. In a first stage, the animals were trained to perform behavioral (manual dexterity) tasks until they reached a stable behavioral score (pre-lesion plateau). In the second stage, an incomplete unilateral cervical cord hemisection was performed and the tip of a catheter attached to an osmotic pump was inserted intrathecally at the lesion site. A group of eight animals received a control antibody (14–80 mg/animal), a second group of five animals received an anti-Nogo-A antibody treatment (total: 14.6–36 mg/animal), and a last group of five animals received a combined treatment of anti-Nogo-A antibody (36 mg/animal) and BDNF (1.4 mg/animal). The treatments were initiated immediately after the lesion and lasted 1 month.

In a third stage, starting immediately after the lesion, each animal was assessed behaviorally until it reached a stable score (post-lesion plateau). In the fourth stage, the anterograde tracer biotin dextran amine (BDA) was injected into the contralesional motor cortex. In some animals, a dextran–fluorescein tracer was injected in the ipsilesional motor cortex. After about 2 months, delay to allow anterograde transport of the tracers, the animals were sacrificed. In this report, the code identifying each animal is built in two parts: the first letters of the code indicate the treatment given (**Mk-C** for the control antibody treatment, **Mk-A** for the anti-Nogo-A antibody treatment, **Mk-AB** for the combined anti-Nogo-A antibody/BDNF treatment) and the additional letter(s) individuate the corresponding animal. The experimenter was blind as to the treatment of the animals and a different identification code was used during the whole duration of the experimental period. The final identification code was set after the sacrifice of the animals when the lesion was reconstructed and some of the behavioral and anatomical data analyzed.

Histology (BDA/SMI-32/dextran–fluorescein staining)

When the animals had reached a stable behavioral score post-lesion, approximately 100 days following the lesion, the BDA tracer was injected unilaterally in the contralesional motor cortex (hand territory) using Hamilton syringes (Table 1). After

transport time (Table 1), the animals were sacrificed as follows. First, the monkeys were sedated with ketamine. Then, they received a lethal injection of sodium pentobarbital (90 mg/kg) intraperitoneally. They were then perfused transcardially with 0.4 l of saline (0.9%), followed by 3 l of a fixative solution (4% of paraformaldehyde in 0.1 M of phosphate buffer, pH 7.6). The perfusion continued subsequently with two solutions of similar fixative containing sucrose of increasing concentrations (10%, 20%) and ended with a 30% sucrose solution in phosphate buffer (pH 7.6). At the end of the perfusion, the entire CNS was isolated and placed during few days in a 30% solution of sucrose in phosphate buffer (pH 7.6) for cryoprotection. A spinal cord segment (C3–T4) comprising the lesion was cut parasagittally in either three or five series of respectively 50 or 30- μ m sections and processed to visualize either BDA or SMI-32 staining. More rostral and caudal spinal cord segments were cut in 50- μ m-thick coronal sections and also collected in series. The SMI-32 staining was carried out according to the following protocol: first, to remove the endogenous peroxidase activity, the free-floating sections were preincubated during 10 min in 1.5% H₂O₂ in phosphate-buffered saline (PBS; pH 7.2) and incubated overnight at 4 °C in SMI-32 monoclonal antibody (Sigma, dilution 1:3000) in addition to 2% normal horse serum and 0.2% Triton X-100; then the sections were rinsed several times in PBS. After that, the sections were rinsed several times again and incubated in a biotinylated secondary antibody (1:200, Vector Burlingame, CA, USA) during 30–60 min at room temperature. Finally, the sections were stained with the avidin–biotin complex (ABC) immunoperoxidase method (Vectastain Elite kits, Vector, Burlingame, CA, USA). The reaction was visualized with 3,3'-diaminobenzidine tetrahydrochloride (DAB 0.05%) as the chromogen, diluted in Tris–saline with 0.001% H₂O₂. The sections were then washed, mounted on gelatin-coated slides, dehydrated, and coverslipped. In the present investigation, the number and the cumulative length of the SMI-32 (+) fibers visible in the lesion site were assessed at 400 \times magnification using a light microscope (Olympus) and the software Neurolucida (MicroBrightField, Williston, VT, USA). The sections analyzed in the present study were used previously in some of the monkeys to reconstruct the location and the extent of the cervical lesion in previous reports (Schmidlin et al., 2004; Wannier et al., 2005; Freund et al., 2009). Finally, for nine animals (five control antibody-treated; one anti-Nogo-A antibody-treated and three anti-Nogo-A antibody/BDNF-treated) the SMI-32-positive fibers' thickness (diameter) was measured.

Treatments

Three different purified IgG antibodies (concentrated to 3.7–10 mg/ml in PBS) were used in the present study. The antibodies were delivered intrathecally at the site of the lesion via a catheter attached to an osmotic pump (Alzet 2M2 or 2M4). The pumps were placed in the back of the animal and the treatment started within minutes following the spinal cord lesion. After about 30 days, the pumps were removed. The control antibody corresponds to a mouse monoclonal antibody directed against wheat auxin (AMS Biotechnology, Oxon/UK) and it was administered up to a total amount of 14–36 mg in eight animals. The anti-Nogo-A antibody (14–36 mg) delivered during 4 weeks to four animals (Table 1) corresponded to a mAb hNogo-A monoclonal antibody which recognizes a defined Nogo-A region of the human Nogo-A sequence. The monkey Mk-AF (Table 1) received a monoclonal antibody (11C7; 14 mg in 4 weeks) directed against a rat Nogo-A sequence of 18 amino acids (aa623–640) which builds a strong inhibitory region of the Nogo-A protein. On Western blots, both anti-Nogo-A antibodies can identify in a nonspecific manner the primate-Nogo-A protein (Oertle et al., 2003; Weinmann et al., 2006). The question of whether the two types of anti-Nogo-A

antibodies present a difference in efficacy was not addressed in the present study because only one animal was treated with the 11C7 type of anti-Nogo-A antibody. Five animals (Mk-ABBo, Mk-ABMa, Mk-ABMx, Mk-ABP and Mk-ABS) have received the anti-Nogo-A antibody treatment (36 mg in 4 weeks), combined to 1.4 mg of the neurotrophic factor BDNF (Peprotech, UK) diluted in artificial CSF (150 mM Na, 3 mM K, 1.4 mM Ca, 0.8 mM Mg, 1 mM P, 155 mM Cl) and delivered intrathecally from a second similar osmotic pump caudally to the lesion site during the same period of 4 weeks (Table 1).

For statistics, we compared the diameter distribution of fibers in the lesion territory with that of motoneurons' axons using the Student's *t*-test. For assessing whether the number or the length of the fibers inside the lesion site were affected in one of the groups that received growth-promoting substances, we performed multivariate nonparametric analysis using the R program (R Development Core Team, 2008) with the MNM package (Klaus Nordhausen et al., 2009). This approach uses a nonparametric multivariate rank test (Oja and Randles, 2004) and is equivalent to the approach we used in a previous report (Freund et al., 2009).

RESULTS

Cervical cord lesion

All the animals were subjected to an incomplete spinal cord hemisection at the level of the transition between the segments C7 and C8. The lesions sites were clearly identifiable in all animals and reconstructed from the histological sections. Their relative size was determined as a proportion (in percent) of the extent of the hemi-cord cross-sectional surface (Table 1) and was always clearly identifiable. The lesion extent ranged between 38% and 95% of the hemicord surface. In nearly all monkeys, the lesion completely interrupted the dorsolateral funiculus, spared large portions of the dorsal columns and spread in the ventral quadrant. Two representative histological reconstructions of the spinal cord lesion are shown in Fig. 2.

Which spinal elements are labeled by SMI-32 staining?

The SMI-32 antibody recognizes an epitope on non-phosphorylated neurofilaments, which is only expressed by specific categories of neurons (Sternberger and Sternberger, 1983; Campbell and Morrison, 1989). We identified and analyzed thin and large SMI-32 (+) fibers in all animals, without any particular individual difference of distribution in the lesion site. Cross sections from intact spinal cord tissue segments located rostrally to the spinal cord lesion and stained for SMI-32 revealed that among spinal neurons, motoneurons were the most heavily stained (Fig. 1A, F, white arrowheads). Other SMI-32-stained neurons are scattered across the entire gray matter but only few of them were as heavily stained as motoneurons (Fig. 1E, white arrowhead). In the white matter, lightly stained axons were often visible, as for instance in the dorsal funiculus (Fig. 1B), in the dorsal root entry zone (Fig. 1C) or in the dorsolateral funiculus (Fig. 1D), whereas heavily stained axons were rare, with the exception of axons present in the spino-cervical tract (Fig. 1C). Motoneuronal axons in

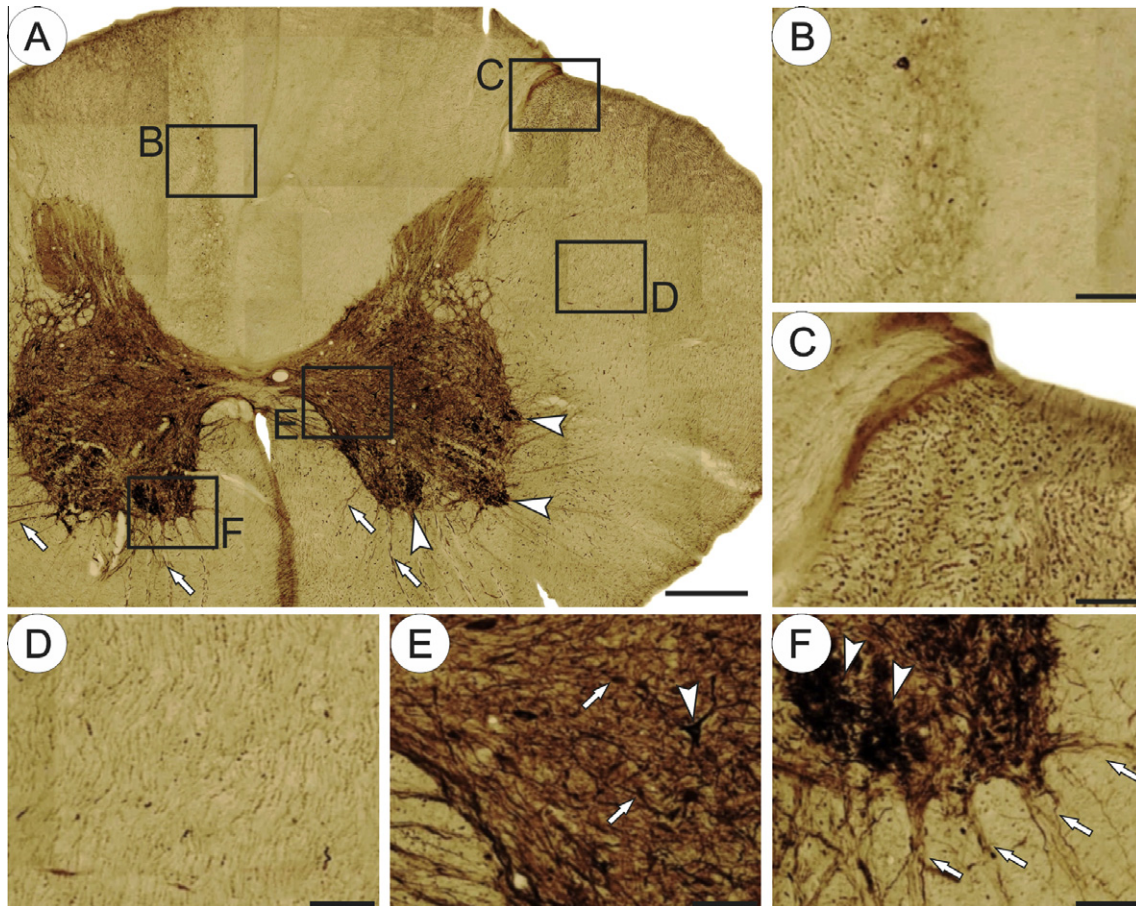


Fig. 1. Distribution of SMI-32-stained elements inside the spinal cord. (A) SMI-32-stained coronal section from a level rostral to the cervical lesion. The gray matter is easily distinguishable from the white matter and presents numerous sites with darkly stained elements. In particular, in the ventral gray matter, strongly stained pools of motoneurons are well recognizable (white arrowheads; F). In the white matter, apart from bundles of fiber spreading in the plane of the section (white arrows), no conspicuous elements are seen. (B) At higher magnifications, lightly stained SMI-32 (+) fibers can be seen in the left portion of this microphotograph in the dorsal columns. This portion is in the region containing ascending axons which have not been sectioned by the lesion. On the right of the microphotograph, which corresponds to a region where axons have degenerated after the lesion, no such staining is found. (C) Numerous well-stained SMI-32 (+) fibers are present in the posterior spinocerebellar tract. (D) Moderately stained SMI-32 (+) fibers are present in the dorsolateral funiculus. (E) The gray matter is filled with a fine mesh of SMI-32 (+) neuropile components in which few large (white arrowhead) and frequent small (white arrows) positively stained cell bodies are disseminated. (F) The motoneurons pools (white arrowheads) build the only sites where numerous heavily stained SMI-32 (+) neurons are grouped. Scale bars = (A) 500 μm and (B–F) 100 μm .

the white matter were also heavily stained (Fig. 1A, F, white arrows).

SMI-32-stained fibers in the lesion territory

The number of SMI-32-stained fibers in the lesion territory varied from a total of 129 counted fibers in Mk-AF to a maximal value of 2539 fibers in Mk-CH (Table 1). Fig. 2 depicts two SMI-32-stained longitudinal sections of the spinal cord at the lesion site. In the first section, the lesion extends through the entire dorso-ventral axis (Fig. 2A). In the gray matter adjacent to the lesion, numerous fibers and many neurons can be seen (Fig. 2A). Heavily stained neurons with a large cell body are concentrated in the adjacent ventral gray matter, most of them are most likely corresponding to motoneurons (Fig. 2A, arrowheads). Numerous large caliber SMI-32 (+) fibers grow into and are present in the lesion site (Fig. 2B, black arrowheads), some of

which can unequivocally be recognized as motoneuron axons, as they are prolongations of motoneuronal axon bundles from the intact white matter (Fig. 2B, arrows). Fig. 2C and D depicts a section from another animal located at a more medial position than in the upper panels of Fig. 2. In this section, the lesion occupies only the ventral part of the spinal cord (Fig. 2C). Here too, numerous SMI-32 (+) fibers are found in the lesion territory. In all animals, the fiber growth did not follow a specific orientation (Fig. 2B, D) and only few exceptions were observed to bridge the rostro-caudal extent of the lesion (Fig. 2D, black arrowhead).

Do CS fibers contribute to the SMI-32 (+) fibers present in the lesion site?

To clarify whether CS fibers are present and common among the SMI-32 (+) fibers detected in the lesion, SMI-32-stained sections were compared to adjacent

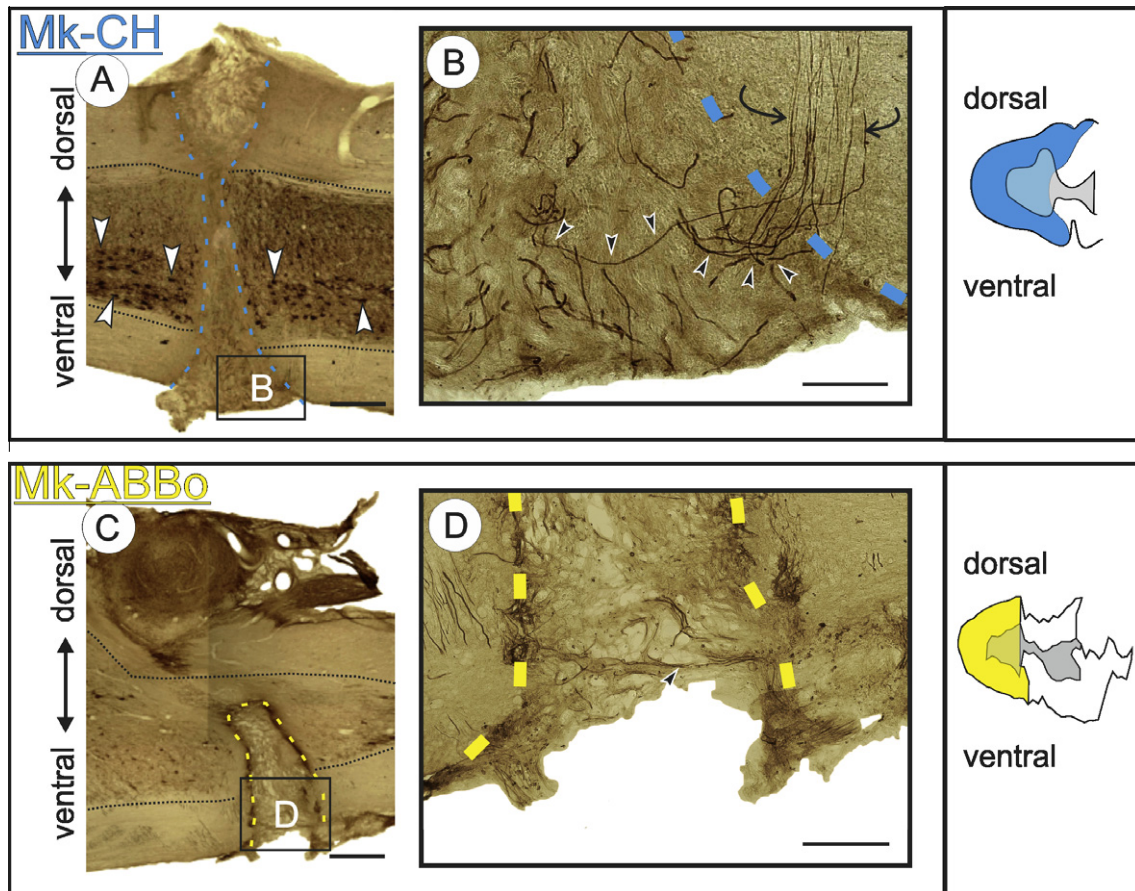


Fig. 2. SMI-32-stained elements inside the lesion territory. (A) SMI-32-stained longitudinal section of the spinal cord at the level of the lesion. The material originates from a monkey that received the control antibody (Mk-CH). The limits of the lesion are indicated by the blue-dashed lines and the limits of the gray matter are shown with black-dotted lines. The lesion extends throughout the entire dorso-ventral axis. The large darkly stained SMI-32 (+) neurons that accumulate in the ventral part of the gray matter are mostly motoneurons (white arrowheads). (B) Enlargement of the zone marked by a rectangle in (A). Numerous SMI-32 (+) fibers are visible in the lesion territory (arrowheads) and in the nearby intact white matter (curved arrows). These last fibers form a bundle of darkly stained fibers running in a plane orthogonal to the axis of the spinal cord. Thus bundles are typical of motoneurons axons crossing the white matter to exit the spinal cord and form ventral roots. Note that these fibers do not change noticeably their diameter as they cross the border between the intact tissue and the lesion. (C) SMI-32-stained longitudinal section of the spinal cord at the level of the lesion. The material originates from a monkey that received the combination of the anti-Nogo-A antibody and BDNF (Mk-ABBo). The limits of the lesion are indicated by the yellow-dashed line and the limits of the gray matter are shown with black-dotted lines. At this level, the lesion extends only throughout the ventral portion of the spinal cord. (D) Enlargement of the zone marked by a rectangle in (C). Numerous SMI-32 (+) fibers are visible in the lesion site. Most fibers grow erratically inside the lesion site, but a few fibers may keep a fixed orientation across the rostro-caudal extent of the scar (black arrowhead). Drawings on far right represent the histological reconstructions of the lesions of the cervical cord on frontal sections of the corresponding animals.

sections processed for BDA only, the tracer that was injected before sacrifice of the animals into the primary motor cortex. Numerous darkly BDA-stained CS fibers are visible in the dorsolateral funiculus rostrally to the cervical lesion (Fig. 3B). Thus, the progression of the CS fibers is clearly stopped at the rostral border of the lesion site (Fig. 3C). As described before, numerous SMI-32 (+)-stained fibers were seen in the lesion site (Fig. 3D), particularly in its ventral portion (Fig. 3F). In contrast, BDA (+)-stained fibers were not found in the corresponding regions of the adjacent BDA-processed sections (Fig. 3E, G). These data show that the overwhelming majority of the SMI-32 (+) fibers observed in the lesion territory do not comprise CS axons.

What is the origin of the SMI-32 (+) fibers visible in the lesion site?

As described above, SMI-32 (+) motoneuronal axons are sometimes clearly seen to penetrate in the scar tissue (Fig. 2B) but the question remains as to whether other fiber populations also significantly contribute to the population of SMI-32 densely labeled fibers found in the lesion territory. We measured the diameter of the SMI-32 (+) axons in the lesion site and compared it to that of the SMI-32 (+) motoneuronal axons in the intact white matter. Individual fibers, analyzed either in the intact white matter or in the lesion site (Fig. 2B), exhibited a comparable diameter distribution independently of the

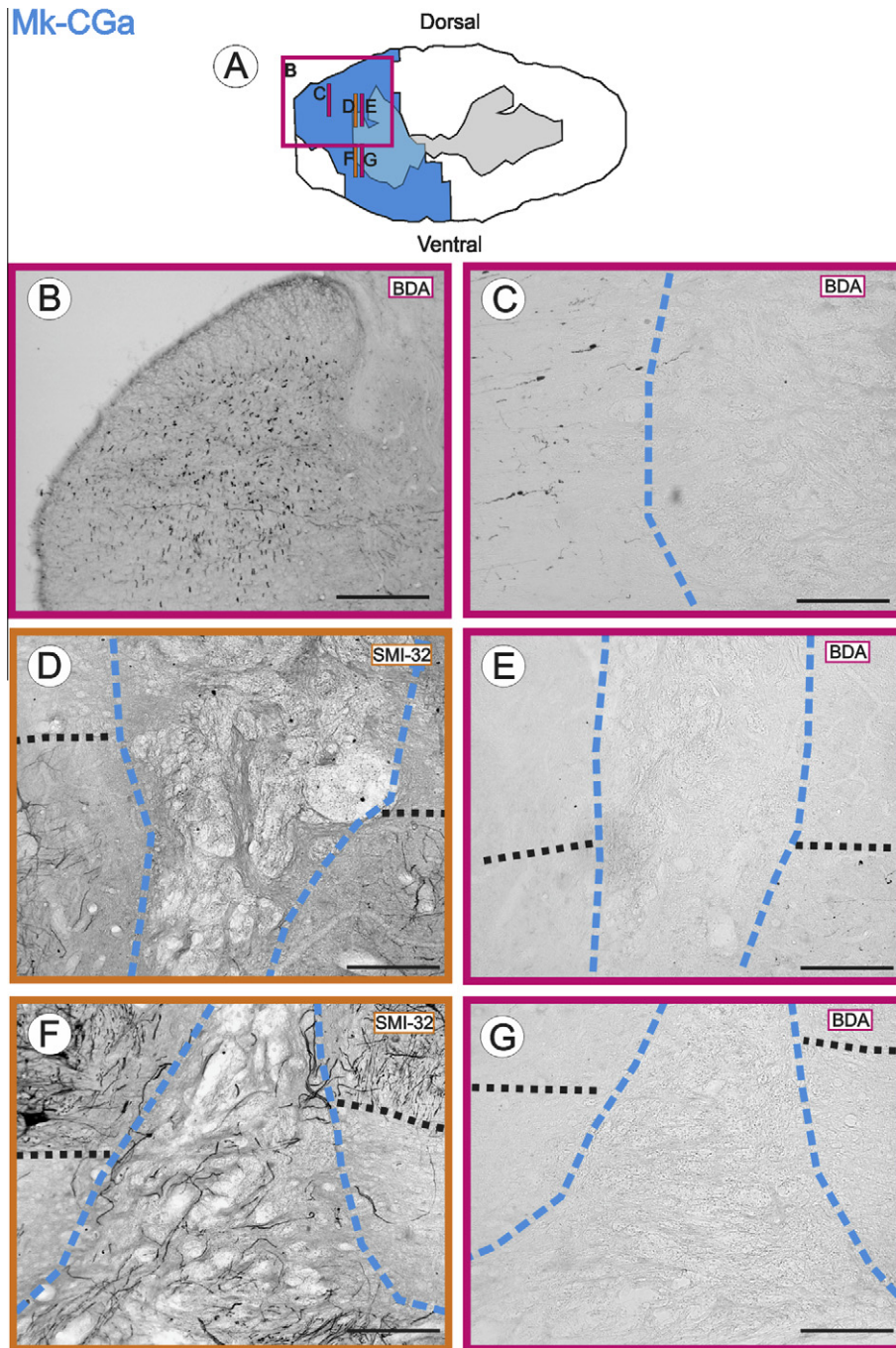


Fig. 3. The SMI-32-stained elements inside the scar tissue are not CS axons. (A) Reconstruction of the spinal lesion in monkey Mk-CGa, illustrating the localization inside the spinal cord of the photomicrographs illustrated in panels (B)–(G). (B) Coronal section located immediately rostrally to the spinal cord lesion stained for BDA and showing a large number of darkly stained CS tract fibers in the dorsolateral funiculus. (C) Section stained for BDA at the level of the dorsolateral funiculus. CS axons normally barely penetrate inside the lesion site. (D) In the lesion territory at the level of the dorsal horn, few SMI-32 (+) fibers can be seen. (E) Section adjacent to that depicted in (D) and stained for BDA. Note the absence of BDA (+) fibers in and outside of the lesion. (F) In the lesion territory at the level of the ventral horn, numerous SMI-32 (+) fibers can be seen. (G) Section adjacent to that depicted in (F) and stained for BDA. Note here also the absence of BDA (+) fibers in and outside of the lesion site. In (C)–(G) photomicrographs, the limits between the intact and the lesioned tissue are indicated by blue-dashed lines and the limits between the white and the gray matter are shown with black-dotted lines. Scale bars = (B) 500 μm and (C–G) 250 μm .

region where the measure was performed, showing that the diameter of motoneuronal axons did not change after they crossed from the intact tissue into the lesion. In the latter, both thick and thin SMI-32 (+) fibers were found,

however (Fig. 4A). The thick fibers were usually heavily stained with the SMI-32 antibody (Fig. 4A, white arrowhead) and looked similar to motoneuronal axons in the intact white matter. Other fibers were rather thin and

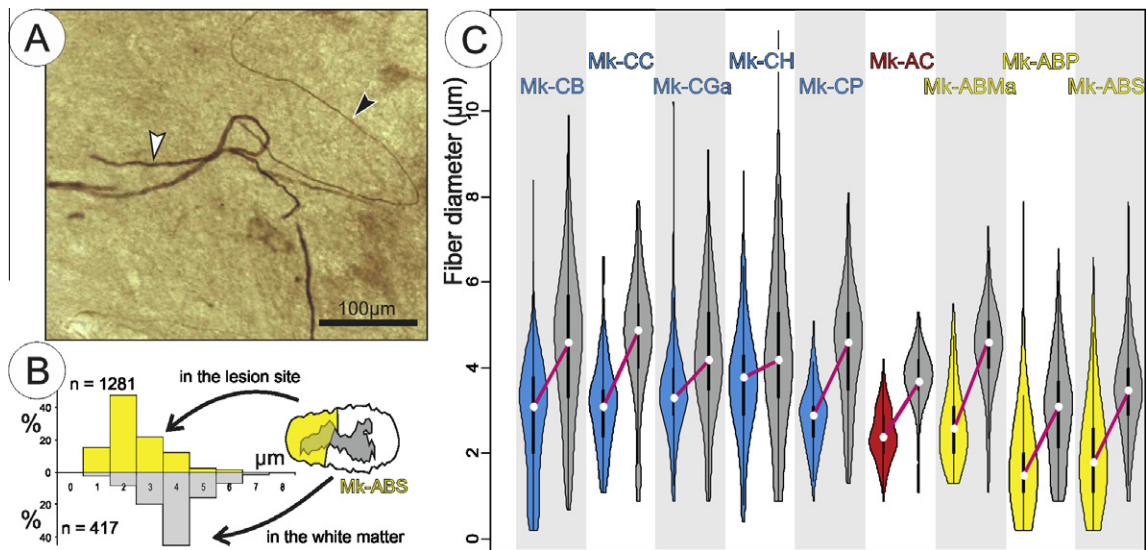


Fig. 4. Distribution of the SMI-32-stained fibers' thickness in the lesion and in the intact white matter. (A) In the lesion territory, the diameter of SMI-32 (+) fibers differs: some fibers are rather thick and densely stained (white arrowhead) and some fibers are rather thin and less densely stained (black arrowhead). (B) Diameter distribution of the SMI-32 (+) fibers observed inside the lesion site (yellow) and into the motoneuronal axons bundles inside the intact white matter (gray) of one animal (Mk-ABS). Note that though largely overlapping, the comparison of both distributions shows that motoneuronal axons are generally large and cannot account for all SMI-32 (+) fibers found inside the lesion site. (C) Comparisons of the SMI-32 (+) fibers diameter distributions for nine animals (in the lesion site in color versus intact tissue in gray). The violin plots indicate the median (white point), the first and third quartiles (thicker line segment), the minimum and maximum of the data as well as the distribution of the observations (envelope). A red segment line connects the median of the data obtained from one animal. Note that for all animals, the median diameter of fibers inside the lesion is always lower than the median diameter of motoneurons axons inside the intact white matter. A statistical comparison between both fibers' populations conducted for each animal using the Student's *t*-test indicated that the difference in diameter was statistically significant for all animals ($p < 0.001$).

less densely stained (Fig. 4A, black arrowhead), features that are exceptional for motoneuronal axons inside the intact white matter. For the monkey Mk-ABS, the diameter distribution of the SMI-32 (+) fibers in the scar tissue was compared to that of the motoneuronal axons outside the scar. Both distributions overlapped, but the proportion of small diameter fibers was higher in the lesion site (Fig. 4B). This difference in fiber distribution was consistently observed in all animals for which diameter measurements were obtained (Fig. 4C; $N = 9$) and was statistically significant in all cases (Student's *t*-test, $p < 0.01$). The data thus suggest that motoneuronal axons are not the only fibers having the capacity to invade the scar tissue.

Do SMI-32 (+) fibers present in the lesion territory respond to the growth-promoting treatments?

To clarify whether the growth of SMI-32 (+) fibers into the lesion territory was affected by the presence of the anti-Nogo-A antibody, combined or not with BDNF, we counted the number of SMI-32 (+) fibers and measured their cumulative length inside the lesion territory. The number of SMI-32 (+) fibers counted in the lesion site varied considerably across the 18 animals (Fig. 5A) and tended to increase in relation to the size of the lesion (Fig. 5B). Comparing the group of animals that received the control antibody to those that received the anti-Nogo-A antibody using a multivariate nonparametric analysis failed to show an influence of the treatment on the growth of the fibers in the scar ($p > 0.05$). The

same was observed when comparing the group of animals which received the control antibody to those that received the combination of BDNF and the anti-Nogo-A antibody.

SMI-32 (+) fibers in the lesion territory belong presumably mainly to motoneurons, but since the thinner fibers inside the lesion did not have counterparts inside the motoneuronal axon bundles in the intact white matter, these thin fibers were probably not belonging to motoneurons. By investigating separately the effects of the treatments on the largest and on the thinnest fibers, we tried to assess whether the treatments could have acted differently on different populations of neurons. Considering the distribution of the fibers' thickness (Fig. 4B, C), we arbitrarily chose the limit of $1.3 \mu\text{m}$ to separate the entire population into a group of thin fibers that, presumably, were predominantly not motoneuronal axons and a group of large fibers for which the proportion of motoneuronal axons is large. The percentage of SMI-32 (+) fibers having a diameter of less than $1.3 \mu\text{m}$ was then plotted against the extent of the hemi-cord lesion (Fig. 5C). As for the total number of SMI-32 (+) fibers (Fig. 5A), a large variability was observed across animals and, here too, a multivariate nonparametric analysis failed to disclose any effect of the treatments on these thin fibers.

It was also conceivable that the SMI-32 (+) fibers increased in length, while their number remained constant. The length of all fiber segments found in the scar tissue was thus measured and summed into a single cumulated value for each animal. Plotting the

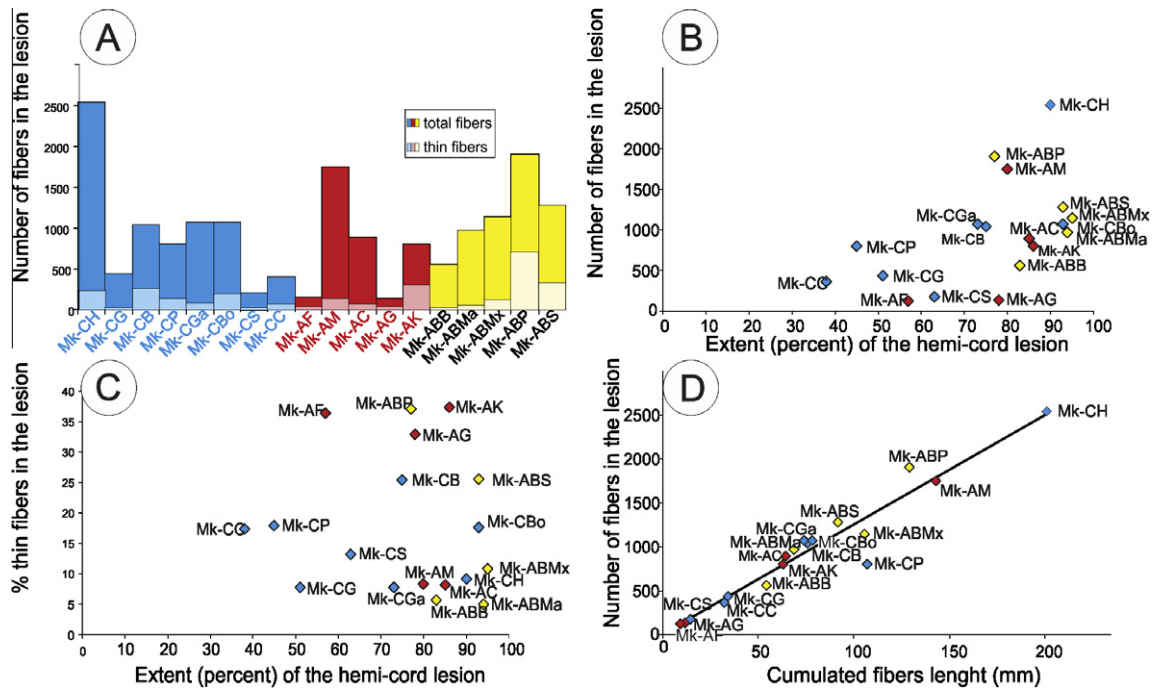


Fig. 5. The number or cumulate length of SMI-32 (+) fibers inside the lesion site are influenced neither by the anti-Nogo-A antibody nor applied together with BDNF. (A) Bargraph representing the total number of SMI-32 (+) fibers counted in the scar tissue for each animal and each treatment. For all animals, the bar is divided in a lower region filled with a light color and corresponding to the fibers with a diameter lower than $1.3 \mu\text{m}$, and a upper region filled with a darker color and corresponding to the larger fibers (see text). Note that a large individual variability is present in all three groups of animals and that the variability is equally important for the thin and the thick fibers. No difference between treatment groups can be detected. (B) Number of fibers counted in the lesion site plotted as a function of the extent of the lesion and showing that this is not the sole result of the lesion extent. No difference between treatment groups was detected. (C) Percentage of fibers thinner than $1.3 \mu\text{m}$ counted in the lesion site plotted as a function of the extent of the lesion and showing that for these fibers too, the variability is not accounted for by the extent of the lesion and that no difference between treatment groups was detected. (D) Number of fibers counted in the lesion territory plotted as a function of their cumulated length and showing that the growth of fibers is not affected by the treatments. Blue: control antibody-treated animals; yellow: anti-Nogo-A/BDNF-treated animals.

number of SMI-32 (+) fibers found in each animal in relation to their cumulated length revealed a linear relationship (Fig. 5D), which was confirmed by high coefficients of correlation ($r > 0.93$) for each experimental group considered separately, as well as for all animals pooled together. In this situation too, the multivariate nonparametric analysis did not disclose any difference between the groups that could be related to the treatments. Again, this tendency was independent from the diameter of the fibers. Thus, it appears that neither the number nor the length of the SMI-32 (+) fibers observed in the scar tissue was influenced by the anti-Nogo-A antibody alone or in combination with the neurotrophic factor BDNF.

DISCUSSION

We analyzed the lesion territory of 18 adult macaque monkeys in the cervical spinal cord, 3.5–8.5 months after a lateral hemisection lesion. Some of the animals underwent growth and regeneration-promoting treatments, i.e. intrathecal infusion of anti-Nogo-A antibodies (for 1 month after the lesion) with or without BDNF. Here we observed that a sizeable amount of neurites was found in the lesion territory. The bulk of these neurites presumably originated from motoneuronal

axons, but it is likely that axons of other origins, though not of corticospinal neurons, also contributed to some extent. The growth of these fibers into the lesion site was affected neither by the presence of the anti-Nogo-A antibody, nor by the presence of a mixture of this antibody with BDNF.

SMI-32-stained elements inside the spinal cord

The scar tissue formed after a spinal cord lesion is known to hinder the growth of nerve fibers into the lesion (Ramon y Cajal, 1928; Brown and MacCouch, 1947; Clemente, 1955; Reier et al., 1983; Stichel and Muller, 1998; Fawcett and Asher, 1999; Shearer and Fawcett, 2001; Silver and Miller, 2004; Fawcett, 2006). In the present study, 129–2539 SMI-32 (+) fibers were found within the lesion site of all the animals. Indirect evidence suggests that a large proportion of these fibers are motoneuronal axons. First, in spinal cord sections, strongly stained SMI-32 (+) neurons were, for a majority, motoneurons; none of the SMI-32 (+)-descending or -ascending axons present in the white matter showed such a darkly stained appearance. Second, many of the strongly SMI-32 (+) fibers in the lesion exhibited a large diameter, characteristic of motoneurons' axons. Third, motoneuronal axons

crossing from the intact adjacent white matter into the lesion could be seen. Nevertheless, axons of thinner caliber were also present and probably represent non-motoneuronal fibers.

Comparisons between the SMI-32 (+) neurons and those expressing choline acetyltransferase revealed that 82–100% of the positive neurons located in the ventral horn of rats and primates (marmoset and rhesus monkeys) were double-stained. However, the SMI-32 staining is not specific for motoneurons. It also stains, though often less densely, neurons outside the ventral horn, such as for instance neurons in the Clark's columns or in the intermediate cell column (Carriado et al., 1996; Tsang et al., 2000). Our observations are in accordance with those reports. As shown in Figs. 1 and 2, the majority of the darkly SMI-32-stained neurons was located in the motoneuronal pools of the ventral horn. Other strongly SMI-32-stained neurons were detected in positions corresponding to Rexed laminae V–VIII, but they were clearly less numerous.

In the cat, intraspinal sprouting of motoneuron axons was observed after root avulsions and spinal cord injuries (Linda et al., 1985, 1992; Havton and Kellerth, 1987). Regeneration included the production of axon-like processes from dendrites and that were called “dendraxons” (Linda et al., 1985, 1992; Havton and Kellerth, 1987). These axons were myelinated, oriented toward the ventral root fascicles and kept a constant diameter. Although the existence of dendraxons has, at least to the best of our knowledge, never been reported in the primate, we cannot exclude that some of the SMI-32 (+) fibers observed here in the lesion site are “dendraxons”.

CS fibers fail to grow inside scar tissue

In a previous report on macaques that had been treated with either a control antibody or the anti-Nogo-A antibody during 1 month after injury, CS fibers were only exceptionally found to penetrate into the lesion site (Freund et al., 2007). This observation is confirmed here in four additional animals receiving the control antibody and in two animals treated with the anti-Nogo-A antibody. We also show that, in five animals that received a combination of the anti-Nogo-A antibody together with BDNF, the number of fibers' numbers in the lesion territory were not different from those found in the non-treated monkeys. In rodents, the absence of axotomized CS fibers in the lesion has repeatedly been observed (Schnell and Schwab, 1990; Bregman et al., 1995; Inman and Steward, 2003) and in primates (Fouad et al., 2004; Freund et al., 2006). In these species, while a treatment neutralizing Nogo-A often leads to enhanced sprouting and regeneration of axotomized CS fibers, the fibers grow around the lesion instead of through the lesion. Interestingly, spontaneous invasion of the lesion site occurs by dorsal root afferents like those containing the calcitonin gene-related peptide (CGRP) or Substance P, and by serotonergic-descending fibers which were reported to cross the inhibitory boundary formed by reactive astrocytes and to penetrate deeply into the scar (De Castro et al., 2005).

In addition, neurites containing glycine and GABA were also found within spinal scars (Brook et al., 1998). Recently, it has been shown that the axons of adult cat's spinal commissural interneurons can spontaneously grow through a local midline spinal section in spite of the presence of CSPGs in the lesion site and that these axons formed functional synaptic connections with appropriate neural targets (Fenrich and Rose, 2009). It thus appears that the mammalian spinal scar tissue does not constitute an environment hostile to regeneration for all fiber types. While this is firmly established for rodents and cats (Matthews et al., 1979; Linda et al., 1985, 1992; Havton and Kellerth, 1987; Wallace et al., 1987; Wang et al., 1996; Brook et al., 1998; Fenrich and Rose, 2009, 2011), it has, to our knowledge, never been reported for adult macaque monkeys. Our data show that SMI-32 (+) fibers may even be attracted by the scar tissue, to invade the lesion site.

Possible impact of the invasion of motoneuronal neurites in the scar

Compared to the 400,000 axons in the corticospinal tract of macaque monkeys, the relatively important number of fibers observed here in the lesion may have a positive impact on supraspinal control of movement and consequently on the functional recovery. Nevertheless, their chaotic distribution in the spinal cord could impair efficient CS neurites to grow in the scar tissue and rewire the motor centers to the motoneurons. Confronting the present morphological data with the percentage of functional recovery (Table 1), there was no relationship between number of fibers in the lesion territory or their cumulative lengths and the functional recovery.

Anti-Nogo-A antibody treatment alone or combined with BDNF does not induce detectable changes in the number or growth of the SMI-32 (+) fibers in the lesion territory

The SMI-32 (+) fibers encountered in the spinal lesion in the present investigation demonstrate that this tissue is growth permissive for some types of neuronal fibers. Nogo-A is not expressed in the scar tissue of rodents, but it was of interest to ascertain whether or not an antibody treatment neutralizing Nogo-A or an additional delivery of BDNF would enhance the growth of SMI-32 (+) fibers inside the lesion territory. However, we did not detect any growth-promoting effect of these treatments on the SMI-32 (+) fibers into the lesion site. Finally, independent of the treatments and the thickness of the fibers, a great variability of the number and length of the fibers in the scar was observed across all animals; local properties of the scar and its interface with the surrounding gray and white matter tissue may account for this variability, but the underlying molecular mechanisms remained to be analyzed.

Acknowledgments—The authors wish to thank the technical assistance of Véronique Moret, Françoise Tinguely, Christiane

Marti, Monika Bennefeld and Christine Roulin (histology), Josef Corpataux, Bernard Morandi, Bernard Bapst and Laurent Bossy (animal house keeping), André Gaillard (mechanics), Bernard Aebischer (electronics), Laurent Monney (informatics). They also would like to thank Dr. Patrick Freund and Dr. Tanja Kakebeeke. This research was supported by grants from The Swiss National Science Foundation (Grant Nos.: 31-43422.95, 31-61857.00, 310000-110005, 31003A-132465, 31003A-132465 (E.M.R.), 31-63633 (M.S.), 4038043918/2 (PNR-38), PZ00P3-121646 (E.S.) and 3100A0-104061, 310000-118357 (T.W.)). The National Centre of Competence in Research (NCCR) "Neural plasticity and repair" of the SNSF, and The Christopher Reeves Foundation Spinal Cord Consortium, (Springfield, NJ). The anti-Nogo-A antibody has been provided by Novartis©.

REFERENCES

- Beaud ML, Schmidlin E, Wannier T, Freund P, Bloch J, Mir A, Schwab ME, Rouiller EM (2008) Anti-Nogo-A antibody treatment does not prevent cell body shrinkage in the motor cortex in adult monkeys subjected to unilateral cervical cord lesion. *BMC Neurosci* 9:5.
- Bregman BS, Kunkel-Bagden E, Schnell L, Dai HN, Gao D, Schwab ME (1995) Recovery from spinal cord injury mediated by antibodies to neurite growth inhibitors. *Nature* 378:498–501.
- Brook GA, Plate D, Franzen R, Martin D, Moonen G, Schoenen J, Schmitt AB, Noth J, Nacimiento W (1998) Spontaneous longitudinally orientated axonal regeneration is associated with the Schwann cell framework within the lesion site following spinal cord compression injury of the rat. *J Neurosci Res* 53:51–65.
- Brown JO, MacCouch GP (1947) Abortive regeneration of the transected spinal cord. *J Comp Neurol* 87:131–137.
- Campbell MJ, Morrison JH (1989) Monoclonal antibody to neurofilament protein (SMI-32) labels a subpopulation of pyramidal neurons in the human and monkey neocortex. *J Comp Neurol* 282:191–205.
- Carriedo SG, Yin HZ, Weiss JH (1996) Motor neurons are selectively vulnerable to AMPA/kainate receptor-mediated injury in vitro. *J Neurosci* 16:4069–4079.
- Clemente CD (1955) Structural regeneration of neuroglia and connective tissue. In: Windle WF, editor. *Regeneration in the central nervous system*. Springfield: Charles C. Thomas. p. 147–161.
- David S, Lacroix S (2003) Molecular approaches to spinal cord repair. *Annu Rev Neurosci* 26:411–440.
- Davies SJ, Fitch MT, Memberg SP, Hall AK, Raisman G, Silver J (1997) Regeneration of axons in white tracts of the central nervous system. *Nature* 390:680–683.
- Davies SJA, Goucher DR, Doller C, Silver J (1999) Robust regeneration of adult sensory axons in degenerating white matter of the adult rat spinal cord. *J Neurosci* 19:5810–5822.
- De Castro Jr R, Tajrishi R, Claros J, Stallcup WB (2005) Differential responses of spinal axons to transection: influence of the NG2 proteoglycan. *Exp Neurol* 192:299–309.
- Fawcett JW (2006) Overcoming inhibition in the damaged spinal cord. *J Neurotrauma* 23:371–383.
- Fawcett JW, Asher RA (1999) The glial scar and central nervous system repair. *Brain Res Bull* 49:377–391.
- Fenrich KK, Rose PK (2009) Spinal interneuron axons spontaneously regenerate after spinal cord injury in the adult feline. *J Neurosci* 29:12145–12158.
- Fenrich KK, Rose PK (2011) Axons with highly branched terminal regions successfully regenerate across spinal midline transections in the adult cat. *J Comp Neurol* 519:3240–3258.
- Fouad K, Klusman I, Schwab ME (2004) Regenerating corticospinal fibers in the Marmoset (*Callithrix jacchus*) after spinal cord lesion and treatment with the anti-Nogo-A antibody IN-1. *Eur J Neurosci* 20:2479–2482.
- Freund P, Schmidlin E, Wannier T, Bloch J, Mir A, Schwab ME, Rouiller EM (2006) Nogo-A-specific antibody treatment enhances sprouting and functional recovery after cervical lesion in adult primates. *Nat Med* 12:790–792.
- Freund P, Schmidlin E, Wannier T, Bloch J, Mir A, Schwab ME, Rouiller EM (2009) Anti-Nogo-A antibody treatment promotes recovery of manual dexterity after unilateral cervical lesion in adult primates – re-examination and extension of behavioral data. *Eur J Neurosci* 29:983–996.
- Freund P, Wannier T, Schmidlin E, Bloch J, Mir A, Schwab ME, Rouiller EM (2007) Anti-Nogo-A antibody treatment enhances sprouting of corticospinal axons rostral to a unilateral cervical spinal cord lesion in adult macaque monkey. *J Comp Neurol* 502:644–659.
- Havton L, Kellerth JO (1987) Regeneration by supernumerary axons with synaptic terminals in spinal motoneurons of cats. *Nature* 325:711–714.
- Inman DM, Steward O (2003) Ascending sensory, but not other long-tract axons, regenerate into the connective tissue matrix that forms at the site of a spinal cord injury in mice. *J Comp Neurol* 462:431–449.
- Nordhausen K, Mottonen J, Oja H (2009) MNM: Multivariate Nonparametric Methods. An approach based on spatial signs and ranks. R package version 0.95-1.
- Lee VM, Otvos Jr L, Carden MJ, Hollosi M, Dietzschold B, Lazzarini RA (1988) Identification of the major multiphosphorylation site in mammalian neurofilaments. *Proc Natl Acad Sci U S A* 85:1998–2002.
- Liebscher T, Schnell L, Schnell D, Scholl J, Schneider R, Gullo M, Fouad K, Mir A, Rausch M, Kindler D, Hamers FPT, Schwab ME (2005) Nogo-A antibody improves regeneration and locomotion of spinal cord-injured rats. *Ann Neurol* 58:706–719.
- Linda H, Cullheim S, Risling M (1992) A light and electron microscopic study of intracellularly HRP-labeled lumbar motoneurons after intramedullary axotomy in the adult cat. *J Comp Neurol* 318:188–208.
- Linda H, Risling M, Cullheim S (1985) 'Dendraxons' in regenerating motoneurons in the cat: do dendrites generate new axons after central axotomy? *Brain Res* 358:329–333.
- Maier IC, Ichiyama RM, Courtine G, Schnell L, Lavrov I, Edgerton VR, Schwab ME (2009) Differential effects of anti-Nogo-A antibody treatment and treadmill training in rats with incomplete spinal cord injury. *Brain* 132:1426–1440.
- Matthews MA, St Onge MF, Faciane CL, Gelderd JB (1979) Axon sprouting into segments of rat spinal cord adjacent to the site of a previous transection. *Neuropathol Appl Neurobiol* 5:181–196.
- McKeon RJ, Schreiber RC, Rudge JS, Silver J (1991) Reduction of neurite outgrowth in a model of glial scarring following CNS injury is correlated with the expression of inhibitory molecules on reactive astrocytes. *J Neurosci* 11:3398–3411.
- Oertle T, Van der Haar ME, Bandtlow CE, Robeva A, Burfeind P, Buss A, Huber AB, Simonen M, Schnell L, Brosamle C, Kaupmann K, Vallon R, Schwab ME (2003) Nogo-A inhibits neurite outgrowth and cell spreading with three discrete regions. *J Neurosci* 23:5393–5406.
- Oja H, Randles RH (2004) Multivariate nonparametric tests. *Stat Sci* 19:598–605.
- Pasterkamp RJ, Verhaagen J (2001) Emerging roles for semaphorins in neural regeneration. *Brain Res Brain Res Rev* 35:36–54.
- R Development Core Team (2008) A language and environment for statistical computing, Vienna, Austria.
- Ramon y Cajal S (1928) *Degeneration and regeneration of the nervous system* (May RM, translator). New York: Oxford UP.
- Reier PJ, Stensaas LJ, Guth L (1983) The astrocytic scar as an impediment to regeneration in the central nervous system. In: *In the spinal cord reconstruction*. New York: Raven Press. p. 163–195.
- Rudge JS, Silver J (1990) Inhibition of neurite outgrowth on astroglial scars in vitro. *J Neurosci* 10:3594–3603.
- Schmidlin E, Wannier T, Bloch J, Belhaj-Saif A, Wyss A, Rouiller EM (2005) Reduction of the hand representation in the ipsilateral

- primary motor cortex following unilateral section of the corticospinal tract at cervical level in monkeys. *BMC Neurosci* 6:56.
- Schmidlin E, Wannier T, Bloch J, Rouiller EM (2004) Progressive plastic changes in the hand representation of the primary motor cortex parallel incomplete recovery from a unilateral section of the corticospinal tract at cervical level in monkeys. *Brain Res* 1017:172–183.
- Schnell L, Schwab ME (1990) Axonal regeneration in the rat spinal cord produced by an antibody against myelin-associated neurite growth inhibitors. *Nature* 343:269–272.
- Schwab ME (2002) Repairing the injured spinal cord. *Science* 295:1029–1031.
- Schwab ME (2004) Nogo and axon regeneration. *Curr Opin Neurobiol* 14:118–124.
- Schwab ME (2010) Functions of Nogo proteins and their receptors in the nervous system. *Nat Rev Neurosci* 11:799–811.
- Schwab ME, Bartholdi D (1996) Degeneration and regeneration of axons in the lesioned spinal cord. *Physiol Rev* 76:319–370.
- Shearer MC, Fawcett JW (2001) The astrocyte/meningeal cell interface – a barrier to successful nerve regeneration? *Cell Tissue Res* 305:267–273.
- Silver J, Miller JH (2004) Regeneration beyond the glial scar. *Nat Rev Neurosci* 5:146–156.
- Sternberger LA, Sternberger NH (1983) Monoclonal antibodies distinguish phosphorylated and nonphosphorylated forms of neurofilaments in situ. *Proc Natl Acad Sci U S A* 80:6126–6130.
- Stichel CC, Muller HW (1998) The CNS lesion scar: new vistas on an old regeneration barrier. *Cell Tissue Res* 294:1–9.
- Thallmair M, Metz GAS, Z'Graggen WJ, Raineteau O, Kartje GL, Schwab ME (1998) Neurite growth inhibitors restrict plasticity and functional recovery following corticospinal tract lesions. *Nat Neurosci* 1:124–131.
- Tsang YM, Chiong F, Kuznetsov D, Kasarskis E, Geula C (2000) Motor neurons are rich in non-phosphorylated neurofilaments: cross-species comparison and alterations in ALS. *Brain Res* 861:45–58.
- Wallace MC, Tator CH, Lewis AJ (1987) Chronic regenerative changes in the spinal cord after cord compression injury in rats. *Surg Neurol* 27:209–219.
- Wang ZH, Walter GF, Gerhard L (1996) The expression of nerve growth factor receptor on Schwann cells and the effect of these cells on the regeneration of axons in traumatically injured human spinal cord. *Acta Neuropathol* 91:180–184.
- Wannier T, Schmidlin E, Bloch J, Rouiller EM (2005) A unilateral section of the corticospinal tract at cervical level in primate does not lead to measurable cell loss in motor cortex. *J Neurotrauma* 22:703–717.
- Wannier-Morino P, Schmidlin E, Freund P, Belhaj-Saif A, Bloch J, Mir A, Schwab ME, Rouiller EM, Wannier T (2008) Fate of rubrospinal neurons after unilateral section of the cervical spinal cord in adult macaque monkeys: effects of an antibody treatment neutralizing Nogo-A. *Brain Res* 1217:96–109.
- Weinmann O, Schnell L, Ghosh A, Montani L, Wiessner C, Wannier T, Rouiller E, Mir A, Schwab ME (2006) Intrathecally infused antibodies against Nogo-A penetrate the CNS and downregulate the endogenous neurite growth inhibitor Nogo-A. *Mol Cell Neurosci* 32:161–173.

(Accepted 22 September 2012)
(Available online 2 October 2012)